Mol Neurobiol (2016) 53:7237–7253
DOI 10.1007/s12035-015-9582-7

Expression of Iron-Related Proteins at the Neurovascular Unit Supports Reduction and Reoxidation of Iron for Transport Through the Blood-Brain Barrier

Annette Burkhart[1] · Tina Skjørringe[1] · Kasper Bendix Johnsen[1] · Piotr Siupka[2] · Louiza Bohn Thomsen[1] · Morten Schallburg Nielsen[2] · Lars Lykke Thomsen[3] · Torben Moos[1]

Received: 17 August 2015 / Accepted: 29 November 2015 / Published online: 21 December 2015

Abstract The mechanisms for iron transport through the blood-brain barrier (BBB) remain a controversy. We analyzed for expression of mRNA and proteins involved in oxidation and transport of iron in isolated brain capillaries from dietary normal, iron-deficient, and iron-reverted rats. The expression was also investigated in isolated rat brain endothelial cells (RBECs) and in immortalized rat brain endothelial (RBE4) cells grown as monoculture or in hanging culture inserts with defined BBB properties. Transferrin receptor 1, ferrireductases Steap 2 and 3, divalent metal transporter 1 (DMT1), ferroportin, soluble and glycosylphosphatidylinositol (GPI)-anchored ceruloplasmin, and hephaestin were all expressed in brain capillaries in vivo and in isolated RBECs and RBE4 cells. Gene expression of DMT1, ferroportin, and soluble and GPI-anchored ceruloplasmin were significantly higher in isolated RBECs with induced BBB properties. Primary pericytes and astrocytes both expressed ceruloplasmin and hephaestin, and RBECs, pericytes, and astrocytes all exhibited ferrous oxidase activity. The coherent protein expression of these genes was demonstrated by immunocytochemistry. The data show that brain endothelial cells provide the machinery for receptor-mediated uptake of ferric iron-containing transferrin. Ferric iron can then undergo reduction to ferrous iron by ferrireductases inside endosomes followed by DMT1-mediated pumping into the cytosol and subsequently cellular export by ferroportin. The expression of soluble ceruloplasmin by brain endothelial cells, pericytes, and astrocytes that together form the neurovascular unit (NVU) provides the ferroxidase activity necessary to reoxidize ferrous iron once released inside the brain.

Keywords Endothelial · Ceruloplasmin · DMT1 · Ferroportin · Hephaestin · Pericyte

Abbreviations

ACM	Astrocyte-conditioned medium
α-SMA	Alpha-smooth muscle actin
BBB	Blood-brain barrier
bFGF	Basic fibroblast growth factor
BSA	Bovine serum albumin
CNS	Central nervous system
DAPI	4′,6-Diamidino-2-phenylindole dihydrochloride
Dcytb	Duodenal cytochrome b
DMT1	Divalent metal transporter 1
GFAP	Glial fibrillary acidic protein
GPI	Glycophosphatidylinositol
MTP1	Metal transporter protein 1
NVU	Neurovascular unit
PBS	Phosphate-buffered saline
PDGFRβ	Platelet derived growth factor receptor β
RBE4	Immortalized rat brain endothelial cell line
RBECs	Rat brain endothelial cells
TEER	Trans-endothelial electrical resistance
Tf	Transferrin
Steap	Six-transmembrane epithelial antigen of prostate

✉ Annette Burkhart
abl@hst.aau.dk

[1] Laboratory of Neurobiology, Biomedicine Group, Department of Health Science and Technology, Aalborg University, Fr. Bajers Vej 3B, 1.216, 9220 Aalborg, Denmark

[2] Department of Biomedicine, Aarhus University, Aarhus, Denmark

[3] Pharmacosmos A/S, Holbæk, Denmark

Introduction

Iron is the most abundant transition metal, and in the brain, it is an essential co-factor for many cellular enzymes involved in mitochondrial respiration, neurotransmitter formation, myelination of axons, and cell division [1–4]. Extensive research has revealed several of the molecular mechanisms involved in maintaining iron homeostasis in mammalian non-neuronal tissues, but the cellular and intercellular mechanisms underlying iron uptake and transport within the brain are less understood. In order to obtain transport into the brain, iron must pass through brain endothelial cells and their intermingling tight junctions that constitute the blood-brain barrier (BBB). The brain endothelial cells are surrounded by pericytes and astrocytes that form the neurovascular unit (NVU), which provides structural and inductive support [5]. The BBB prevents macromolecules of the blood plasma including iron-containing transferrin from entering the brain, and mechanisms to elucidate the iron transport across the BBB and into the brain have received intensive attention during the past decade [1–3].

Two different routes for iron transport through the BBB are mainly considered: (1) One route is characterized by internalization of holo-transferrin followed by detachment of iron from transferrin inside brain endothelial cells with further transport of iron into the brain and recycling of apo-transferrin back to the circulation. This route states that holo-transferrin binds the transferrin receptor expressed luminally by brain endothelial cells and follows receptor-mediated endocytosis in clathrin-coated pits [4]. The pH within the endosomes decreases to around 5.5 due to the presence of proton pumping ATPases. At this low pH, the binding of holo-transferrin to the transferrin receptor is weakened, due to a lower affinity of iron for transferrin resulting in iron release from the holo-transferrin molecule [6, 7]. The release of ferric iron from transferrin is subsequently associated with a reduction of the detached ferric iron to ferrous iron, mediated by the presence of ferrireductases like the six-transmembrane epithelial antigen of prostate (Steap) proteins. Within the endosome, iron is subsequently transported into the cytosol by means of a divalent metal-ion transporter (DMT1) [8]. DMT1 is only able to transport ferrous iron, which emphasizes the need for ferrireductases within the endosomes [4, 9]. Ferroportin, also known as metal transport protein 1 (MTP1), is expressed at the surface of cells involved in iron transport and is able to facilitate efflux of ferrous iron across the cell membrane [10]. Within the CNS, two copper-containing proteins are suggested to provide oxidation of ferrous iron, namely ceruloplasmin and its homologue hephaestin [11–13]. Astrocytes express both glycophosphatidylinositol (GPI)-anchored and soluble forms of ceruloplasmin [14].

(2) A second route is characterized by transcytosis of holo-transferrin through brain endothelial cells leading to release of iron from the abluminal side into the brain. This theory mainly evolved due to the conflicting observations on whether DMT1 and ferroportin are expressed by brain endothelial cells [15–17]. Although some studies demonstrated transferrin being transported through brain endothelial cells, the quantitative aspects of transferrin transport at the BBB failed to support the idea of transcytosis [1, 16, 18, 19]. Accordingly, in case DMT1 and ferroportin were not operating in brain endothelial cells to transport through the BBB, it was suggested that other factors like citrate and ATP released from astrocytes could be responsible for the detachment of iron from transferrin at the abluminal membrane of the brain endothelial cells, while transferrin and its receptor would undergo recycling to the luminal membrane [1].

Conflicts also arose as data were obtained from intact organisms or in vitro using dedifferentiated, immortalized cell lines. Studies reported presence of ferroportin mRNA and protein in brain endothelial cells in vivo [20, 21] and in vitro [22], but another study failed to confirm these observations [17]. Likewise, conflicting results reported on absence of DMT1 in vivo [16] but presence in vitro in immortalized brain endothelial cells [23]. An intermediate experimental situation is denoted by primary brain endothelial cells, which can be cultured under the influence of molecules secreted from astrocytes to form a tight barrier in vitro [24]. Primary brain endothelial cells are able to maintain many important characteristics of the BBB in vivo even days after in vitro culture, e.g., they exert high transcellular electric resistance and low passive permeability. Contrary to immortalized endothelial cell lines, they also exert low mitotic activity when forming confluence corresponding to brain endothelial cells in vivo [25]. This is of importance when studying expression of proteins related to iron homeostasis, as the iron uptake is dramatically higher when cells are mitotic [26].

The objective of the present work was to examine the expression profile of proteins involved in iron transport at the BBB and NVU. We studied primary rat brain endothelial cells (RBECs) induced to form a BBB in vitro, and we compared their gene and protein expression with those of cells of the immortalized rat brain endothelial cell line (RBE4). Both cell types were studied in situations where they were non-confluent or confluent, with the latter condition intended to mimic the intact BBB. We also examined the expression profile in primary pericytes and astrocytes. In order to quantify and correlate the gene expression to experimental situations with changes in iron status, we also quantified the expression in liver, duodenal enterocytes, intact brain tissue, and isolated brain capillaries from normal-fed, iron-deficient, and iron-reverted rats. Our data demonstrate expression of many proteins related to iron homeostasis, including DMT1 and ferroportin, which supports the notion of receptor-mediated internalization of holo-transferrin followed by transport of non-transferrin bound iron into the brain and retro-endocytosis of apo-transferrin back to the circulation. Our data

also provide evidence for expression of ceruloplasmin and hephaestin in pericytes and astrocytes.

Materials and Methods

Materials

The following reagents were obtained from Sigma-Aldrich (Brondby, Denmark): Percoll (Cat. No. P1644), collagen type IV (Cat. No. C5533), fibronectin (Cat. No. F1141), poly-L-lysine (Cat. No. P6282), heparin (Cat. No. H3149), puromycin (Cat. No. P8833), hydrocortisone (Cat. No. H4001), CTP-cAMP (Cat. No. C3912), 4-(3-butoxy-4-methoxybenzyl)-imidazolidin-2-one (RO-201724) (Cat. No. B8279), 4′,6-diamidino-2-phenylindole dihydrochloride (DAPI) (Cat. No. D9542), rabbit anti-claudin-5 (Cat. No. SAB4200538), mouse anti-alpha-smooth muscle actin (α-SMA) (Cat. No. A5228), ammonium iron(II) sulfate hexahydrate (Cat. No. F3754), 2-(*N*-morpholino)ethanesulfonic acid hydrate, 4-morpholineethanesulfonic acid (MES) (Cat. No. M2933), and 3-(2-pyridyl)-5,6-diphenyl-1,2,4-triazine-*p*,*p*′-disulfonic acid monosodium salt hydrate (Ferrozine) (Cat. No. 160601).

DNase I (Cat. No. 10104159001), collagenase/dispase (Cat. No. 109113), insulin transferrin sodium selenite (Cat. No. 11074547001), and basic fibroblast growth factor (bFGF) (Cat. No. 1363697) were purchased from Roche (Hvidovre, Denmark). The following reagents were from Life Technology (Naerum, Denmark): Alexa Fluor 488-conjugated goat anti-rabbit IgG (Cat. No. A11034), Alexa Fluor 594-conjugated goat anti-mouse IgG (Cat. No. A11032), collagenase II (Cat. No. 17101105), Dulbecco's modified Eagle's medium (DMEM)/F-12 (Cat. No. 31331), DMEM (Cat. No. 21885), and fetal calf serum (Cat. No. 10270). Bovine serum albumin (BSA) (Cat. No. EQBAH62) was from Europa Bioproducts (Cambridge, UK). Plasma-derived bovine serum (Cat. No. 60-00-810) was from First Link (Wolverhampton, UK). Rabbit anti-ferroportin (Cat. No. MTP11-S) and rabbit anti-DMT1 (Cat. No NRAMP-22S) were purchased from Alpha Diagnostics (AH Diagnostics, Aarhus, Denmark). Mouse anti-rat transferrin receptor 1 (TfR1) (CD71, Serotec) (Cat. No. MCA155G) was from Nordic BioSite ApS (Copenhagen, Denmark). Mouse anti-hephaestin antibody (Cat. No. ab56729) was from Abcam, UK. Rabbit anti-platelet-derived growth factor receptor beta (PDGFRβ) (Cat. No SC-432) was from Santa Cruz. Gentamicin sulfate (Cat. No. 17-518Z) was from Lonza Copenhagen (Vallensbaek Strand, Denmark). Fluorescence mounting medium (Cat. No. S3023), rabbit anti-ceruloplasmin (Cat. No. Q0121), and rabbit anti-glial fibrillary acidic protein (GFAP) (Cat. No. Z0334) were purchased from DAKO (Glostrup, Denmark). Phosphate-buffered saline (PBS) (Cat. No. SH3025802) and all reagents for qPCR were obtained from Thermo Scientific (Hvidovre, Danmark), except primers that were synthesized by TAG Copenhagen (Frederiksberg, Denmark). Hanging cell culture inserts (Cat. No. Pirp 15R48) were obtained from Merck Millipore (Hellerup, Denmark) and polyclonal anti-rabbit horseradish peroxidase (HRP) and anti-mouse HRP were from Cell Signalling (BioNordika, Denmark).

In Vivo Studies

We examined the liver, duodenum, brain stem (intact brain tissue), and brain capillaries from adult male Wistar rats aged postnatal (P) P70 days. We obtained these male rats from pregnant rats, fed either a normal diet or a low-iron content diet. Normal mothers were fed a diet with an iron content of 158 mg/kg (Altromin, Germany), while iron-deficient mothers were fed a diet with an iron content of 5.2 mg/kg (Altromin, Germany) for 6 weeks. They were then fertilized with adult breeder males fed a normal diet and maintained on their respective diets. For reversion of the iron deficiency, female rats were injected subcutaneously with iron isomaltoside 1000 (Pharmacosmos, Denmark) at a dose of 80 mg/kg on day E14 and transferred to the normal diet. The mothers were kept on their respective diets until the male pubs were 21 days old, at where the pubs were separated from their mothers. The littermates were fed the same diet as their respective mothers until deeply anesthetized on P70 by subcutaneous injection of 0.5 ml/10 g body Hypnorm/Dormicum (fentanyl/fluanisone mixed with midazolam and sterile water in a ratio of 1:1:2). Subsequently, the chest was opened, the heart exposed, and the circulation emptied for blood by flushing 0.1 M PBS, pH 7.4, through the heart [27]. We then dissected the brain stem (intact brain tissue), liver, and duodenum and rapidly froze the tissue on dry ice or homogenized for RNA isolation as described below. We sampled the proximal 10 mm of the duodenum by cutting it open with scissors followed by a flush in 0.1 M PBS, pH 7.4, and we made a subsequent scraping of the luminal part with razor blade to isolate a preparation enriched in duodenal mucosa. The brain capillaries were isolated from cortex from the same animals using the same procedure for isolation of primary RBEC described in the following section.

Construction of In Vitro Models

Primary cultures of RBECs were prepared from 2- to 3-week-old Sprague Dawley rats [24, 25]. The rats were deeply anesthetized with 0.5 ml/10 g body weight of Hypnorm/Dormicum and the forebrains collected under sterile conditions. We carefully removed the meninges and any visible white matter and cut the cerebral cortices into small pieces. The brain tissue was digested in collagenase II and DNase I for 75 min at 37 °C. Pellets were suspended in 20 % BSA in

DMEM-F12, centrifuged at 1000 G for 20 min, and further digested in collagenase/dispase and DNase I at 37 °C for 50 min. We manually separated the digested microvessel fragments and collected them using a continuous 33 % Percoll gradient. The isolated microvessels were then washed in DMEM-F12 twice and either frozen for later RNA isolation (brain capillaries) or seeded on collagen type IV and fibronectin-coated 35-mm plastic dishes to obtain primary cultures of RBECs. We maintained primary cultures of RBECs in DMEM/F12 supplemented with 10 % plasma-derived bovine serum, bFGF, heparin, insulin, transferrin, sodium, selenite, and gentamicin sulfate (10 μg/ml) and cultured in an incubator with humidified 5 % CO_2/95 % air at 37 °C. To obtain a pure culture of RBECs, puromycin was added to the cell culture medium in a 4 μg/ml concentration for the first 2 to 3 days. We cultured immortalized RBE4 cells [28] in the same medium as the RBECs and examined them in parallel with the primary RBECs. We obtained primary cultures of pericytes by prolonging the culture of the isolated microvessel fragments [24], which we cultured in uncoated dishes in DMEM supplemented with 10 % fetal calf serum and gentamicin sulfate for about 10 days to ensure pericyte proliferation and survival. Primary cultures of astrocytes were obtained from neonatal Sprague Dawley rats [24] from which brains were collected and dissociated pieces of the cerebral cortex through a 40-μm nylon strainer in DMEM supplemented with 10 % fetal calf serum and gentamicin sulfate. We seeded the dissociated cells on poly-L-lysine-coated cultured flasks for about 2 weeks until they reached confluence, by which the cells were either frozen or passaged onto poly-L-lysine-coated 12-well culture plates.

RBE4 cells and RBECs were grown in co-culture with primary astrocytes seeded in poly-L-lysine-coated 12-well plates approximately 2 weeks prior to the co-culture experiments. We seeded the RBE4 cells and RBECs with a cell density of 1×10^5 cells/cm^2 on collagen IV and fibronectin-coated 12-well polyethylene terephthalate, 1.0 μm hanging cell culture inserts. The cells adhered for 24 h before placing the culture inserts in the 12-well plates containing astrocytes. To further stimulate BBB characteristics of the RBE4 cells and RBECs, they were treated with 550 nM hydrocortisone, 250 μM cAMP, and 17.5 μM RO-201724 [29, 30]. Cells used for the gene expression analysis were stimulated with sterile filtered astrocyte-conditioned medium (ACM) instead of astrocytes to ensure that the purified RNA from the cultures only originated from endothelial cells.

Trans-Endothelial Electrical Resistance (TEER) Measurements

We measured the TEER using a Millicell ERS-2 epithelial Volt-Ohm meter and STX01 Chopstick Electrodes (Millipore, Hellerup Denmark). The TEER values were given as Ω cm^2 of coated cell-free culture inserts subtracted the measured TEER values and multiplied with the difference of the area of the culture insert (1.12 cm^2).

Gene Expression Analyses

We performed gene expression analyses on intact brain tissue (brain stem), liver, duodenal mucosa, RBE4 cells, RBECs, pericytes, and astrocytes. We grew the endothelial cells either as monolayers or in the hanging culture inserts, where they form an in vitro BBB model with induced polarity. RNA was extracted from the RBECs 2 days after isolation, when the cells were approximately 70 % confluent. We seeded RBE4 cells on collagen IV-fibronectin-coated 35-mm dishes at a cell density of 30.000 cells/cm^2 and extracted RNA from the cells, when they reached approximately 70 % confluence as well. RNA was extracted from the RBE4 cells and RBECs grown in polarized condition after 2 days of culturing with ACM [29, 30]. We also extracted RNA from frozen cryoprotected vials of astrocytes and pericytes. We furthermore performed gene expression analysis on RNA extracted from isolated brain capillaries, intact brain tissue, liver, and the duodenal mucosa from the normal, iron-deficient, and iron-reversed rats. RNA was extracted using the GeneJET RNA Purification Kit, and the RNA concentration and purity were determined spectrophotometrically with a 260/280 ratio above 1.8. The RNA was subsequently treated with DNase I enzyme according to the manufacturer's protocol to remove traces of genomic DNA. We used 100 ng of each DNA-free RNA sample as a template for RT-qPCR. We carried out cDNA synthesis using RevertAid Premium First Strand cDNA Synthesis Kit, and we used 2.5 ng cDNA and 10 pmol of each primer listed in Table 1 for each qPCR reaction together with the Maxima™ SYBR Green qPCR Master Mix in a reaction volume of 20 μl. We analyzed each sample in triplicates, and non-reverse-transcribed RNA and water served as negative controls. We used beta-actin as a housekeeping/reference gene for normalization purpose. We used Stratagene Mx 3000P™ QPCR System (Agilent Technologies, Horsholm, Denmark) for RT-qPCR. The PCR conditions were 95 °C for 10 min, followed by 40 cycles of 95 °C for 30 s, 60 °C for 30 s, and 72 °C for 30 s. The relative quantities of DNA were calculated in the analyzed samples by the Pfaffl method [31].

Immunocytochemistry

The cells were rinsed in 0.1 M PBS, pH 7.4, and fixed in 4 % paraformaldehyde for 10 min. They were then incubated with 3 % BSA and 0.2 % Triton X-100 in PBS for 30 min at room temperature to block for non-specific binding of primary antibodies. The cells were incubated for 1 h at room temperature under moderate agitation with primary antibodies raised against claudin-5, α-SMA, PDGFRβ, GFAP, transferrin receptor,

Table 1 Primer sequences used for RT-qPCR

Target	Reference sequence	Forward primer	Reverse primer
Transferrin receptor 1	NM_022712.1	TGGATCAAGCCAGATCAGCATTCTC	TTTCTTCCTCATCTGCAGCCAGTTT
Steap 2	NM_001107846.1	GCTTCGTTATTTCCGGATTCCCTGA	TCGAGCTTGGATATTGTTGCTGCAT
Steap 3	NM_133314.1	CTCACTCAACTGGAAGGAGTTCAGC	GAATGTGGGTGGCAGGTAGAACTTG
DMT1	NM_013173.2	GCTTGTTGCTGTCTTCCAAGATGTG	TTCCGTTGGAGAACTCACTCATCAC
Ferroportin	NM_133315	CCCTGCTCTGGCTGTAAAAG	GCACAGGTGGGTTCTTGTTC
Ceruloplasmin GPI-anchored	NM_001270961.1	CAAACGCCTGGAACCTGGTTACTC	ATGTTCCAGGTCATCCTGTAGCTCTG
Ceruloplasmin Soluble	NM_012532.2	GGAATTGGTAATGCCGATGGACAGA	ATTTGTTGCCACTTTGCAGAGTCCT
Hephaestin	NM_133304.1	TAGCTGGCACCTTGATGACAACATT	CAACTCGGGTAAGTTCCCAAAGACA
Hepcidin	NM_053469	GGCAACAGACGAGACAGACT	AACAGAGACCACAGGAGGAA
GFAP	NM_017009.2	ACATCGAGATCGCCACCTACAGGAA	AGGTGGCCTTCTGACACAGATTTGG
α-SMA	NM_031004.2	GAGTGGAGAAGCCCAGCCAGTC	AACAGCCCTGGGAGCATCATCAC
Claudin-5	NM_031701.2	CTACAGGCTCTTGTGAGGACTTGAC	AGTAGGAACTGTTAGCGGCAGTTTG
β-actin	NM_031144.3	CCTCTGAACCCTAAGGCCAACCGTGAA	AGTGGTACGACCAGAGGCATACAGGG

DMT1, ferroportin, hephaestin, and ceruloplasmin. The five latter antibodies were previously used for detection in brain tissue, e.g., [15, 32–36]. The primary antibodies were diluted 1:200 in incubation buffer consisting of 3 % BSA and 0.2 % Triton X-100 in 0.1 M PBS. Omission of primary antibodies and replacement with incubation buffer served as control for the immunoreaction of the primary antibodies. Alexa Fluor 488-conjugated goat anti-rabbit IgG and Alexa Fluor 594-conjugated goat anti-mouse IgG secondary antibodies were used in a dilution of 1:200 in 3 % BSA and 0.2 % Triton X-100 in 0.1 M PBS and incubated for 1 h. Nuclei were stained with DAPI. The cells were mounted on glass slides together with fluorescent mounting medium and examined under a ×40 oil objective (NA.1.3) in a confocal fluorescent microscope using epifluorescence and generated Z-stacks (Carl Zeiss LSM780, Germany). We used ZEN and the ImageJ software to correct captured images for brightness and contrast.

Western Blotting

The commercially available antibodies used for the immunocytochemistry were analyzed for their specificity using Western blotting. The polarized RBECs, pericytes, and astrocytes were lysed in 150 mM NaCl, 2 mM $MgCl_2$, 20 mM $CaCl_2$, 100 mM Hepes, and 1% Triton X-100, pH 7.4, on ice for 30 min. Then, the cells were centrifuged at 13, 000 rpm for 10 min after which the supernatants were collected. The proteins were added with 25 % SDS-PAGE sample buffer and 10 % DTT and analyzed on a 4–12 % SDS gel together with Blue Prestained Marker (BIORAD, Copenhagen, Denmark). The proteins were then blotted to a nitrocellulose membrane using blotting buffer (0.192 M glycine, 0.25 mM Tris base, 20 % EtOH) for 3 h at 200 mA. The membranes were then blocked for non-specific binding of antibodies in 5 % skim milk in TBS with 0.1 % Tween 20, pH 7.6, after which the membranes were incubated with the primary antibodies diluted 1:100–1:1000 in blocking buffer for 1 h at room temperature. The membranes were subsequently washed four times for 5 min in 1 % skim milk in TBS with 0.1 % Tween 20, pH 7.6, before incubation with secondary anti-rabbit HRP or anti-mouse HRP diluted 1:2000 in blocking buffer. Finally, the membranes were washed four times for 5 min in 1 % skim milk in TBS with 0.1 % Tween 20, pH 7.6, before being developed using ECL.

Ferroxidase Assay

The ferroxidase activity was investigated in confluent monolayers of RBECs, pericytes, and astrocytes ($n = 6$) using a protocol adapted from the Kosman group [35]. In brief, the cells were incubated for 1 h in 5 % CO_2/95 % air at 37 °C with freshly prepared 10 μM ferrous ammonium sulfate in 100 mM MES buffer, pH 6.0, after which the MES buffer was collected. The percentage of remaining ferrous iron in the MES buffer was analyzed using 100 μM of the colorimetric indicator Ferrozine, which when complexed with ferrous iron forms a purple color with an absorbance of 550 nm. All assays were corrected for ferroxidase activity in MES buffer added with ferrous ammonium sulfate without the addition of cellular lysate (Fig. 6a).

Statistics

Data from the TEER measurements were analyzed with the GraphPad Prism 5.0 software (GraphPad Software, Inc., CA,

USA) using a one-way analysis of variance (ANOVA) with Tukey's multiple comparisons post hoc test. Data from the relative gene expression analysis were analyzed with the GraphPad Prism 5.0 software using a one-way ANOVA with Dunnett's multiple comparison post hoc test (in vivo data) or a one-way ANOVA with Tukey's multiple comparisons post hoc test (in vitro data).

Results

The transport of iron at the BBB and the expression of proteins related hereto were previously investigated in vivo [15, 16, 20, 32, 37–39] and in cultured immortalized brain endothelial cells [22, 23, 35, 40]. In the present study, we investigated the expression of genes and proteins related to iron transport using isolated brain capillaries, immortalized RBE4 cells, and primary RBECs. Pericytes and astrocytes that together with endothelial cells constitute the NVU were also included in the study, as they probably contribute to the regulation of iron transport into the brain. Initially, we studied isolated brain capillaries and cultured endothelial cells for their expression of cell-specific markers in order to evaluate their purity (Fig. 1). The brain capillaries were isolated from normal-fed, iron-deficient, and iron-reverted rats. At the initial isolation, brain capillaries denote a mixture of all the cells of the NVU, mainly endothelial cells and pericytes [24]. Therefore, we analyzed for gene expression of claudin-5 (endothelial cell marker), α-SMA (pericyte marker), and GFAP (astrocyte marker) and compared with pure cultures of endothelial cells, pericytes, and astrocytes, respectively (Fig. 1). Expectedly, the isolated capillaries predominantly denoted a mixture of endothelial cells and pericytes, which is consistent with the close association of these two cells types at the capillaries in vivo [5]. In contrast, GFAP-containing astrocytes denoted only a minority in the capillary fraction (Fig. 1). To expand on the conclusions made in studies of iron transporting proteins performed in monocultures [23, 35, 40], we also cultured RBE4s and RBECs when they were non-confluent and highly dividing and when they were cultured on hanging filter inserts, polarized, and formed a confluent layer (Fig. 1). We induced the latter by supplementing the culture medium with astrocyte-conditioned medium (ACM) derived from primary rat astrocytes and monitored the TEER value as a measure of the generation of BBB properties. Culturing cells with ACM is important for development of polarized growth with loss of extracellular, passive permeability for low molecular weight molecules, lowering of mitotic activity, and initiation of expression of hallmark genes [25]. The cells used in this study exhibited similar characteristics as recently published [25] with respect to polarization, permeability, and lowered mitotic activity (data not shown).

Fig. 1 Purity of isolated brain capillaries (**a**) and cell cultures (**b**, **c**). **a** ▶ Brain capillaries were isolated from normal, iron-deficient, and iron-reverted rats. Their gene expressions of markers of the neurovascular unit, claudin-5 (endothelial cells), α-SMA (pericytes), and GFAP (astrocytes) were compared with primary rat brain endothelial cells (*RBECs*) to evaluate their purity. The brain capillary fragments consist of endothelial cells and pericytes, which clearly appear judged from the expression of both claudin-5 and α-SMA. In contrast, the capillary fragments are devoid of GFAP. **b** Immortalized RBE4 cells and primary rat brain endothelial cells (*RBECs*) were cultured under non-polarized conditions without having reached confluence or at a confluent stage under the influence of astrocyte-conditioned medium (*+ACM*), by which the cells become polarized and acquire BBB properties with high trans-endothelial electrical resistance (*TEER*) and low passive permeability [25]. In case of the primary RBECs, they also form a tight barrier layer and enter a phase with little or no mitotic activity [25]. Comprehending this notion, the polarized state of the RBECs results in a consistent expression of claudin-5 at the cell–cell junctions and TEER values above 200 Ω cm^2. This is contrasted in RBE4 cells that lack claudin-5 expression both at the gene and protein level and therefore never reach TEER values above 10 Ω cm^2. **c** The purity of isolated pericyte and astrocyte cultures was examined based on their expression of the cell-specific markers α-SMA and GFAP, respectively, and as can be seen both of these markers exert high cell specificity. Data are presented as means ± SEM ($n = 6–9$). $*p < 0.05$, $**p < 0.01$, $***p < 0.001$. *Scale bar* = 10 μm

For gene expression analyses, the stability of the chosen housekeeping gene β-actin was verified by the relationship between the cDNA concentration in each reaction with the C_T value of the housekeeping gene, and this relationship was stable in all cell lines and tissues when the RT-qPCR were performed according to the abovementioned protocol and MIQE Guidelines. When comparing the relationship between the cDNA concentrations within each PCR reaction to the C_T value of β-actin, we found a stable and comparable relationship of 0.13 ± 0.002 in all four cell types independent of culturing conditions, which allowed us to perform statistical analyses on the gene expression level between the different cell types. The stability of actin was additionally found to be unaffected by iron status (not shown).

Expression of claudin-5 was almost absent in RBE4 cells (Fig. 1b), while expression of claudin-5 was significantly higher in the RBECs and highly elevated when cultured under influence of ACM. Supporting this observation, the mean TEER value for RBE4 cells was as low as 6 ± 0.7 Ω cm^2, whereas it was 201 ± 4 Ω cm^2 for RBECs. TEER values above 130 Ω cm^2 indicate a tight cell layer [41]. The RBE4 cells therefore failed to exhibit this BBB characteristic in spite culturing them under the influence of ACM, which was also evident from the lack of claudin-5 protein expression at the cell–cell junctions, especially when compared to the primary cells (Fig. 1b). Primary isolated pericytes and astrocytes were also analyzed for their expression of cell-specific markers to assess their purity (Fig. 1c). Pericytes expressed α-SMA and

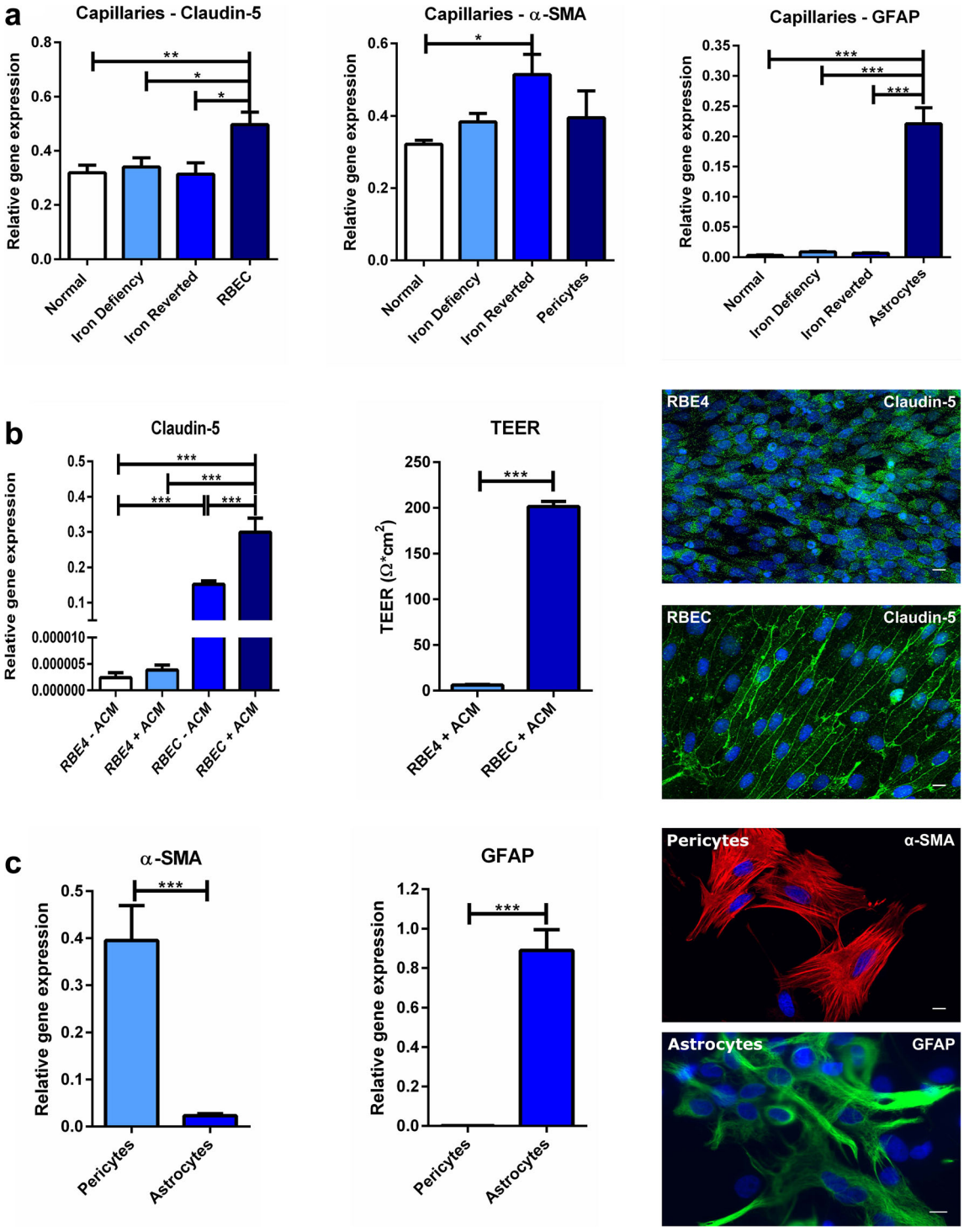

exhibited virtually no expression of the astrocyte marker GFAP. At the protein level, the cells of the pericyte culture correspondingly contained α-SMA-positive pericytes, while the vast majority of cells of the astrocyte culture were GFAP-positive (Fig. 1c). Pericyte contamination was insignificant in the astrocyte preparation.

Endothelial Expression Related to Iron Uptake: Transferrin Receptor 1, Ferrireductases, and DMT1

We then measured the relative expression of genes possibly involved in iron uptake and transport at the BBB (Fig. 2a). Liver, duodenal mucosa, capillaries, and intact brain tissue all

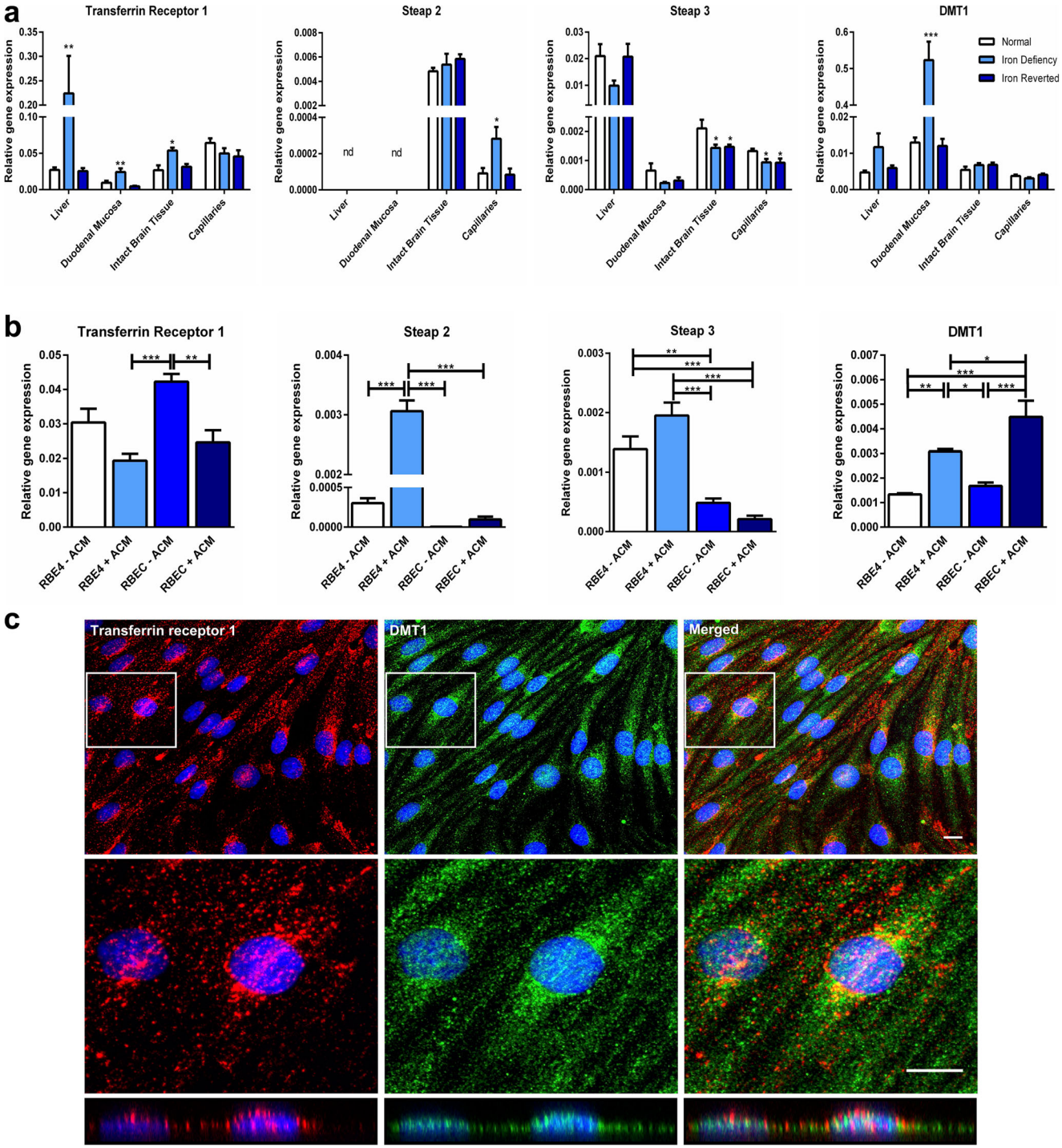

expressed transferrin receptor 1 mRNA. The iron levels in the diet influenced this expression level with an increase in the low-iron group, most prominently observed in liver tissue. In contrast, brain capillaries did not change their expression pattern with changing iron statuses.

Holo-transferrin can undergo uptake and transport at the BBB by receptor-mediated endocytosis and subsequent transport to DMT1-containing endosomes, where iron can detach from transferrin due to a lowering of the pH [42]. An expression of ferrireductases within the endosomes could enable reduction of ferric iron and transport of ferrous iron out of the endosomes by DMT1 [1]. We found that the liver and duodenal mucosa expressed Steap 3 in contrast to Steap 2 (Fig. 2a). The expression of Steap 3 was lowest in the duodenal mucosa, which is also known to express another ferrireductases, duodenal cytochrome b (Dcytb) that may be of significance for reduction of ferric iron to facilitate the intestinal absorption of iron [43]. Brain capillaries and intact

◀ **Fig. 2** Gene and protein expression of molecules related to iron uptake studied in vivo (**a**) and in vitro (**b**, **c**): Transferrin receptor 1 (*TfR1*), ferrireductases (*Steap 2 and Steap 3*), and divalent metal transporter I (*DMT1*). **a** Gene expression was analyzed in liver, duodenal mucosa, intact brain tissue, and purified brain capillaries from normal-fed (*white*), iron-deficient (*light blue*), and iron-reverted (*dark blue*) rats. Transferrin receptor 1 follows the expected pattern with elevated expression in liver, duodenal mucosa, and brain in iron deficiency. Likewise, DMT1 is higher in duodenal mucosa in iron deficiency. *Asterisk* indicates significant differences from normal within the tissues. **b** In brain endothelial cells cultured under non-polarized (−*ACM*) and polarized conditions (+*ACM*), the latter induced by the addition of an astrocyte-conditioned medium (*ACM*), transferrin receptor 1, and DMT1 are seen in all culture conditions. Transferrin receptor 1 is lower and DMT1 higher when cultured under polarized conditions. Steap 2 and 3 are seen in both cell types cultured with the addition of ACM and higher in RBE4 cells than in rat brain endothelial cells (*RBECs*). Data are presented as means ± SEM ($n = 6$–9). *$p < 0.05$, **$p < 0.01$, ***$p < 0.001$. *n.d.*, not detectable. **c** Confocal images reveal the cellular localization of transferrin receptor 1 (*red*) and DMT1 (*green*) in RBECs cultured under polarized conditions. The two cells marked in framed areas are shown in higher magnification (XY plane) and perpendicular hereto (XZ plane). Both proteins are seen on the luminal side above the nucleus. Overlay of the proteins reveals only slight co-localization (XZ plane, *yellow*), and the predominant luminal distribution of transferrin receptor 1 is apparent. Nuclei are stained with DAPI (*blue*). *Scale bar* = 10 μm

brain tissue expressed both Steap 2 and 3. The expression of Steap 2 was very low in the brain capillaries but proved significantly higher in the iron-deficient rats compared to the other dietary groups. The expression of Steap 3 was also very low in the brain capillaries and intact brain tissue. However, it decreased in both tissues at stages of iron deficiency and iron reversion. Liver and duodenal mucosa expressed DMT1 and particularly in the case of the duodenum with an expected increase in DMT1 during iron deficiency [4]. Brain capillaries and intact brain tissue also expressed DMT1 albeit without influence of the different dietary regimens (Fig. 2a).

The gene expression patterns of these proteins related to iron uptake were additionally studied in vitro using the two endothelial cell types and two culturing conditions (Fig. 2b). Expression of the transferrin receptor 1 decreased when the cells were grown under influence of ACM. Expressions of Steap 2 and 3 were increased in the RBE4 cells, and the expression seemed to increase with polarity in both cell types. Both RBE4 and RBECs expressed DMT1, which was increased when grown under influence of ACM (Fig. 2b). Using immunocytochemistry, the protein expression of the transferrin receptor 1 and DMT1 in RBECs cultured under the influence of ACM localized to the cell cytoplasm (Fig. 2c). Z-stack analyses are particularly relevant in cross sections where the nucleus is represented, as this allows for a defined detection of the luminal and abluminal parts [44]. Z-stack analysis of transferrin receptor 1 immunoreactivity revealed that transferrin receptors distributed luminal (on the upper side of the nucleus), which is in good accordance with prior analyses on the subcellular distribution of transferrin receptors in brain endothelial cells in vivo [45]. This distribution hence indicated that the RBECs when grown under influence of the ACM had reached polarization. DMT1 was primarily observed in the luminal part of the cytoplasm. However, when compared to that of the transferrin receptor, which was present very luminally, DMT1 was distributed slightly more profound and nearer the abluminal membrane (Fig. 2c). For the same reason, co-localization of the transferrin receptor and DMT1 was not particularly abundant. Omission of the primary antibodies revealed a lack of cellular immunoreaction. In the Western blotting analysis of the RBEC lysates, both the transferrin receptor and DMT1 were detected at their expected molecular weight levels at approximately 85 and 63 kDa, respectively (data not shown).

As the choice of fixative may affect the distribution of the immunoreaction, we analyzed the distribution of transferrin receptors and DMT1 in the BCECs after fixation with 4 % paraformaldehyde, methanol, or acetic acid. It was not possible to detect differences in the immunoreactivities or the subcellular distribution following application of the different fixatives (data not shown).

Endothelial Expression Related to Iron Export: Ferroportin and Hepcidin

Ferroportin is responsible for the cellular efflux of ferrous iron, and in the case of the brain endothelial cells, this could occur both luminally and abluminally with the latter suggesting a route for iron transport into the brain extracellular space [46]. The possible expression of ferroportin by brain endothelial cells is site of debate [17, 20, 21, 36, 37], but in the recent years, its expression has been documented [21, 35, 40, 46]. We examined the gene expression of ferroportin at the level of the brain capillaries and compared the expression to that found in intact brain tissue, liver, and duodenal mucosa. The expression was highest in liver and duodenum, and the expression was highly increased in the duodenum as a consequence of iron deficiency in good agreement with previous observations [47]. The expression in the brain capillaries was, however, higher than that found in intact brain tissue and was slightly decreased in the iron-deficient animals (Fig. 3a).

Ferroportin is regulated post-translationally by hepcidin [48]. The expression of hepcidin showed the expected changes in liver and duodenal mucosa in response to changes in iron availability [48], whereas there was virtually no expression of hepcidin in intact brain tissue or isolated brain capillaries (Fig. 3a). The expression of ferroportin was highest in polarized cells grown under influence of ACM. Hepcidin was expressed, albeit at very low levels, and its expression significantly increased in polarized RBECs (Fig. 3b). Noteworthy, the expression of hepcidin in RBECs was extremely low compared to that found in the brain capillaries and may be explained by the presence of hepcidin-expressing pericytes in

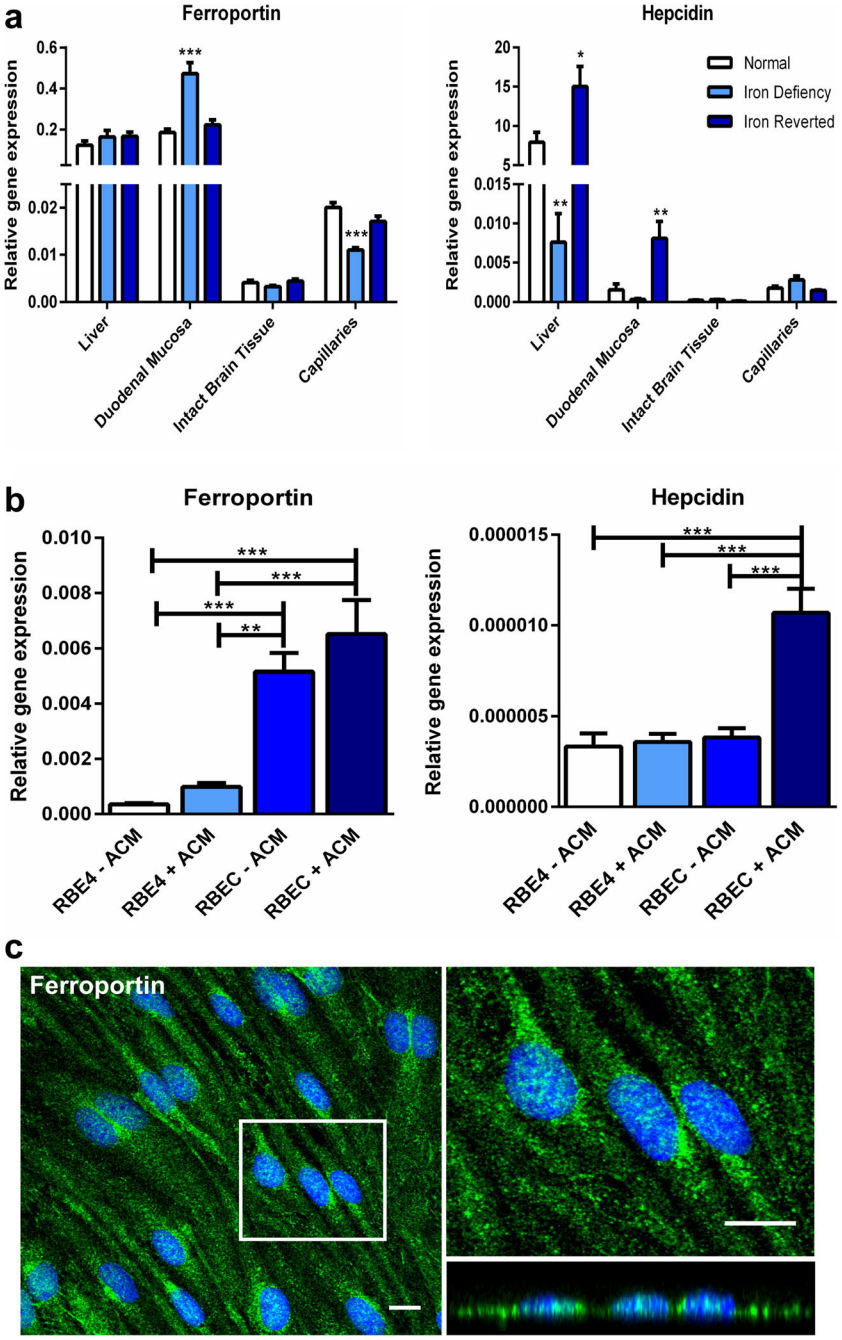

Fig. 3 Expression analyses for molecules related to iron release studied in vivo (**a**) and in vitro (**b**, **c**): Ferroportin and hepcidin. **a** Gene expression was analyzed in liver, duodenal mucosa, intact brain tissue, and purified brain capillaries from normal-fed (*white*), iron-deficient (*light blue*), and iron-reverted (*dark blue*) rats. Ferroportin follows the expected pattern with elevated expression in duodenal mucosa in iron deficiency. Likewise, hepcidin is lower in liver in iron deficiency and higher in duodenal mucosa reverted to the normal diet. Hepcidin transcripts are virtually absent in isolated brain samples. *Asterisk* indicates significant differences from normal within the tissues. **b** In brain endothelial cells cultured under non-polarized (−*ACM*) and polarized states (+*ACM*), the latter induced by the addition of an astrocyte- conditioned medium (*ACM*), ferroportin, and hepcidin are seen in all culture conditions. Ferroportin is higher in brain endothelial cells (*RBECs*) than in RBE4 cells. The number of hepcidin transcripts is so scarce that expression is essentially zero. Data are presented as means ± SEM ($n = 6$–9). *$p < 0.05$, **$p < 0.01$, ***$p < 0.001$. **c** Confocal images reveal the cellular localization of ferroportin in RBECs cultured under polarized conditions. The three cells marked in the framed area are shown in higher magnification (XY plane) and perpendicular hereto (XZ plane). Ferroportin is seen intracellularly with a tendency to distribute to the abluminal membrane. Nuclei are stained with DAPI. *Scale bar* = 10 μm

the capillary fraction (Fig. 5). The possible expression of ferroportin by RBECs cultured with ACM was additionally investigated at the protein level by immunocytochemistry. Ferroportin was observed intracellularly in the cytoplasm with

a tendency to distribute to the abluminal membrane (Fig. 3c). Omission the primary antibodies revealed a lack of cellular immunoreaction. Analysis of the RBEC lysates using Western blotting revealed that ferroportin was detected at its expected molecular weight level at approximately 64 kDa. The antibody reveals another discrete band slightly higher than the expected band at 64 kDa (data not shown). The presence of this band is attributed to post-translational modifications, which have also been observed previously [35, 49].

Endothelial Expression Related to Iron Release: Ceruloplasmin and Hephaestin

Ceruloplasmin and its homologue hephaestin, which both exhibit ferroxidase activity, are candidates for reoxidation of ferrous iron effluxed from the abluminal endothelial cell membrane [11, 50]. Ceruloplasmin exists on both soluble and GPI-anchored forms in astrocytes [14, 51], and endothelial cells are known to express hephaestin [35]. The liver is the source of both forms of ceruloplasmin with the soluble form being much higher expressed than the GPI-anchored form [51], and the duodenum alone expresses the soluble form but at low levels [4, 11]. We made similar observations in our analyses of the liver and duodenal mucosa (Fig. 4a). Brain capillaries and intact brain tissue expressed the two forms of ceruloplasmin. Only the brain capillaries responded to changes in dietary iron via an upregulated expression of the GPI-anchored form in iron deficiency (Fig. 4a). In vitro, the expression of both ceruloplasmin forms was very low compared to that found in the capillaries, which can be explained by that the isolated brain capillary fraction contains ceruloplasmin-expressing pericytes (Fig. 5). The polarized RBEC expressed both forms of ceruloplasmin with the highest expression being the soluble form (Fig. 4b).

Expectedly, the duodenal mucosa was a main source for hephaestin expression (Fig. 4a) with a slight lowered expression in iron-reverted rats [50]. The liver, intact brain tissue, and isolated brain capillaries also expressed hephaestin. In vitro, hephaestin increased in RBE4 and RBECs when cultured with ACM suggesting that increasing the polarity of the endothelial cells led to higher expression (Fig. 4b). Using immunocytochemistry, ceruloplasmin was primarily seen at the cell–cell junctions and in the cytosol of polarized RBECs. Only a vague staining of hephaestin was observed (Fig. 4c). Omission the primary antibodies revealed a lack of cellular immunoreaction. In Western blotting of RBEC lysates, ceruloplasmin but not hephaestin was detected at its expected molecular weight level being approximately 130 kDa (data not shown). However, others, using the same antibody against hephaestin, have previously detected hephaestin in brain endothelial cells at its expected molecular weight in the Western blotting [35].

The Expression of Molecules Related to Iron Release in Pericytes and Astrocytes: Ceruloplasmin and Hephaestin

Due to the close association of pericytes and astrocytes to brain endothelial cells, they are probably also involved in iron transport into the brain [42]. Astrocytes are known sources of both forms of ceruloplasmin [14]. However, since pericytes are in closer proximity with the endothelial cells, they could also contribute to ferrous iron reoxidation. We observed that pericytes expressed both forms of ceruloplasmin to the same extent as that of astrocytes, and we further observed that pericytes expressed hephaestin significantly higher than that of astrocytes (Fig. 5). The pericytes and astrocytes also contained the hepcidin transcript (Fig. 5), which probably accounts for the majority of the expression signal detected in the isolated brain capillaries that invariably also contain pericytes (Fig. 5a). Using immunocytochemistry, both pericytes and astrocytes exhibited ceruloplasmin and hephaestin immunoreactivity (Fig. 5b). Western blotting analysis of pericytes and astrocytes furthermore confirmed the presence of ceruloplasmin in these cell types (data not shown).

Ferroxidase Activity in the Cells of the Neurovascular Unit

The remaining iron content in the MES buffer after exposure to ferrous iron was significantly lowered compared to the control, indicating that the cells had oxidized the added ferrous iron to ferric iron due to the presence of the ferroxidase active proteins ceruloplasmin and hephaestin. Ferroxidase activity was therefore confirmed in all cell types of the neurovascular unit (Fig. 6b). It was not possible to detect significant differences in the ferrous activity between the three cell types.

Discussion

Previous studies on iron transport have mainly been performed in vivo [15, 16, 20, 32, 36–39] or in immortalized RBECs [22, 23, 35, 40]. The in vivo studies can be difficult to interpret as purification of endothelial cells from brain capillaries is complicated and may lead to contamination from irrelevant cell types, hence polluting the data of the gene expression profiling, in particular with the highly sensitive RT-qPCR technique. Immortalized cells lines tend to lose many of their important in vivo like characteristics due to long-term culturing. Primary cells on the other hand are only cultured for one or two passages. The primary cells are able to maintain many of the important in vivo characteristic. They robustly express claudin-5 and readily form a tight barrier making them valid to study the BBB in vitro [30]. When analyzing these primary RBECs, it was evident that they expressed important proteins like DMT1 and ferroportin. The quantitative gene expression of DMT1 and

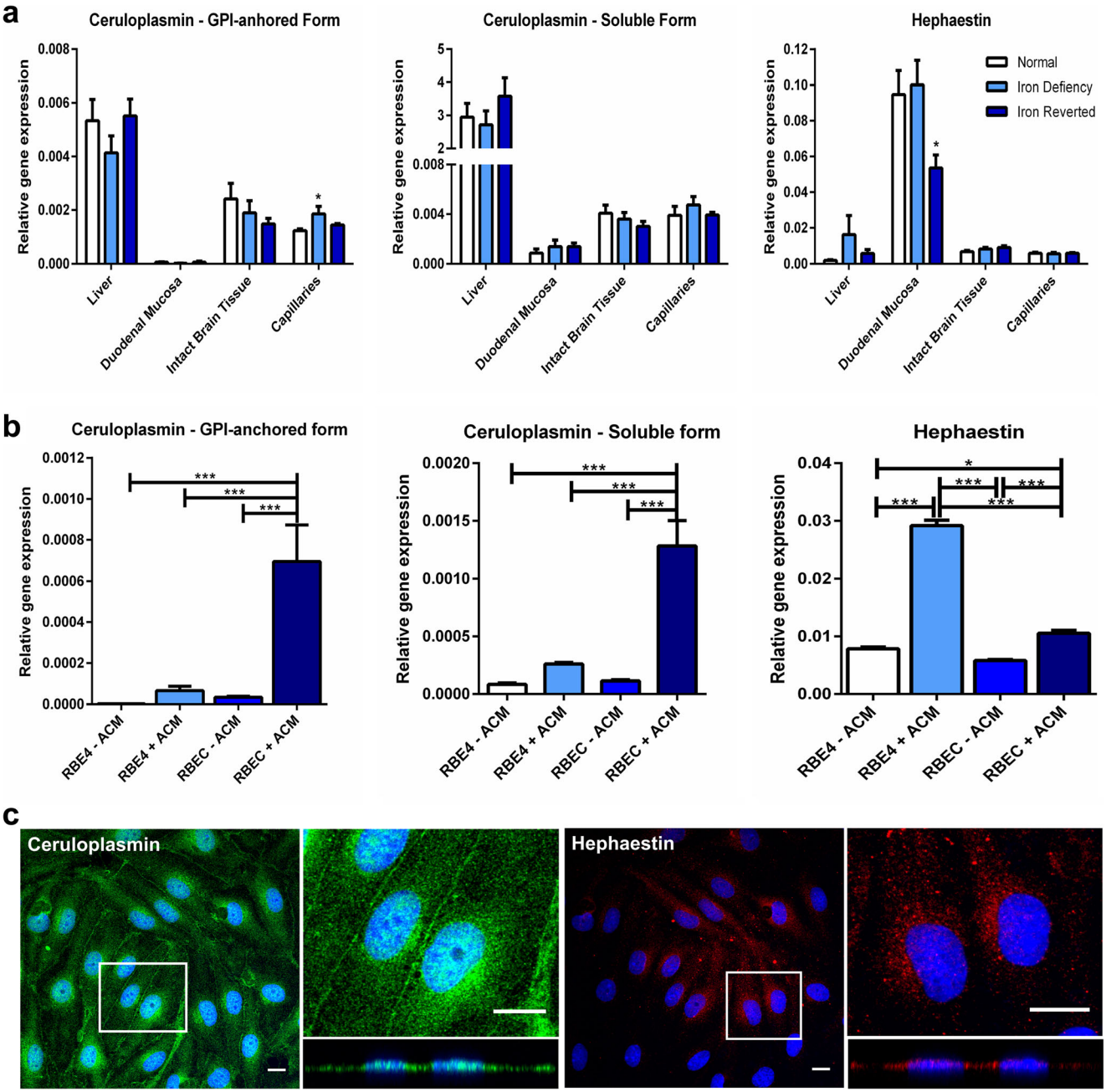

Fig. 4 Gene expression analyses for molecules related to iron release studied in vivo (**a**) and in vitro (**b**, **c**): Ceruloplasmin (GPI-anchored and soluble forms) and hephaestin. **a** Gene expression was analyzed in liver, duodenal mucosa, intact brain tissue, and purified brain capillaries from normal-fed (*white*), iron-deficient (*light blue*), and iron-reverted (*dark blue*) rats. Ceruloplasmin gene expression is high in liver and hephaestin high in duodenal mucosa with a significant lowering when reverted to normal diet. Ceruloplasmin (GPI-anchored and soluble forms) and hephaestin transcripts are all seen in intact brain tissue and in isolated brain capillaries. *Asterisk* indicates significant differences from normal within the tissues. **b** In brain endothelial cells cultured under non-polarized (−*ACM*) and polarized states (+*ACM*), the latter induced by the addition of an astrocyte-conditioned medium (*ACM*), both forms of ceruloplasmin are highest in polarized rat brain endothelial cells (*RBECs*). Notably, the gene expression of hephaestin is higher than that of the ceruloplasmin forms. Data are presented as means ± SEM ($n = 6$–9). $^{*}p < 0.05$, $^{**}p < 0.01$, $^{***}p < 0.001$. **c** Confocal images reveal the cellular localization of ceruloplasmin (*green*) and hephaestin (*red*) in RBECs cultured under polarized conditions. The cells marked in the framed area are shown in higher magnification (XY plane) and perpendicular hereto (XZ plane). Ceruloplasmin is primarily observed at the cell–cell junctions (XY plane) and in the cytosol of RBECs (XZ), while hephaestin exhibits a punctuated distribution in the cytosol. Nuclei are stained with DAPI. *Scale bar* = 10 μm

ferroportin was higher in RBECs than in RBE4 cells, and the expression was at its highest when the RBECs formed the barrier layer. The last observation is signified by the fact that primary RBECs reach a post-mitotic stage when the barrier is forming [25] indicating that the tight barrier is formed by primary post-mitotic RBECs that share great similarity with brain

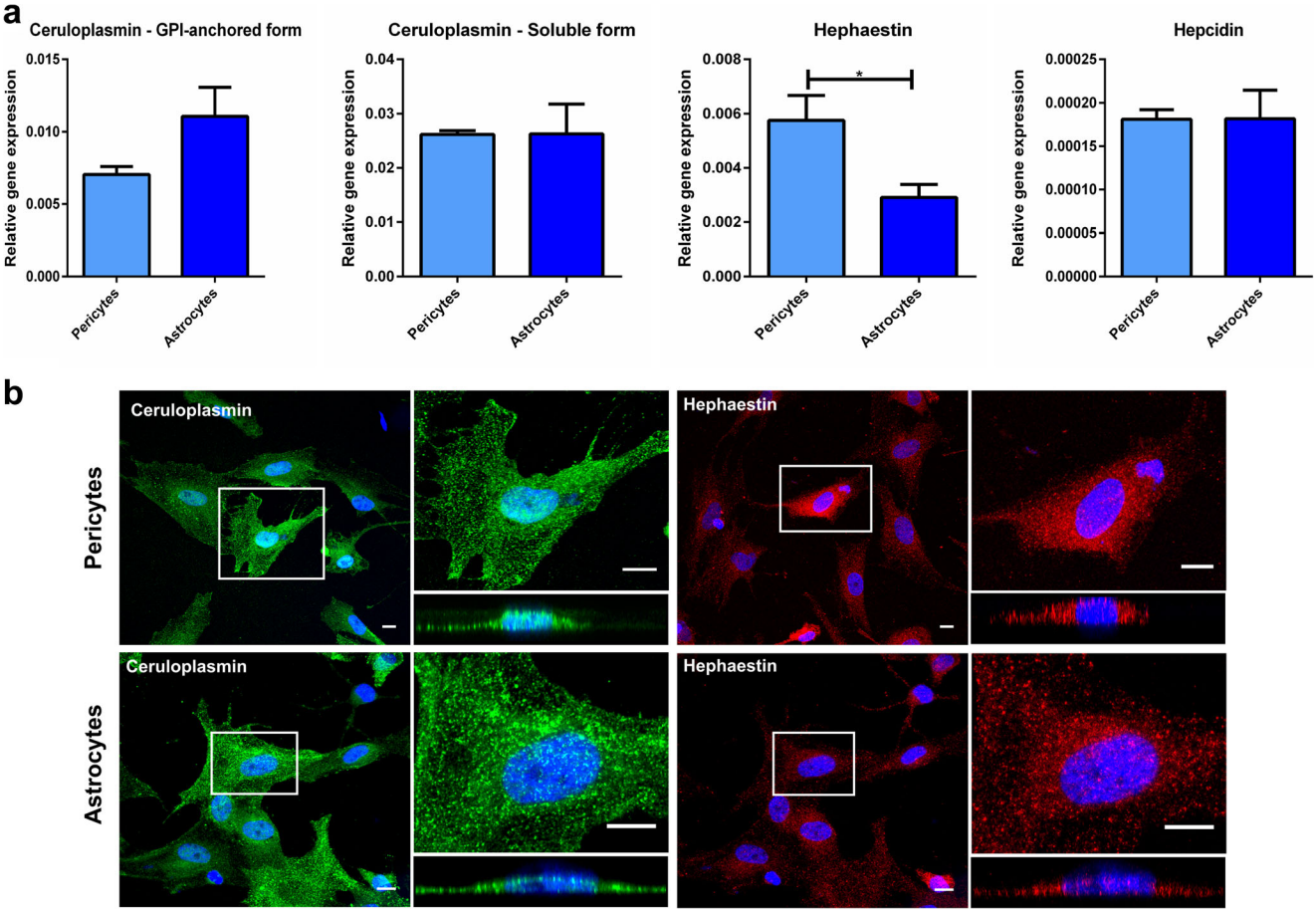

Fig. 5 Expression analyses for ceruloplasmin (GPI-anchored and soluble forms), hephaestin, and hepcidin in primary rat pericytes and astrocytes. **a** Pericytes and astrocytes express both ceruloplasmin forms and hephaestin. By contrast, the number of hepcidin transcripts is so scarce that expression is essentially zero. Data are presented as means ± SEM ($n = 6$). *$p < 0.05$, ***$p < 0.001$. **b** Confocal images reveal the cellular localization of ceruloplasmin (*green*) and hephaestin (*red*) in pericytes and astrocytes. The cells marked in the framed area are shown in higher magnification (XY plane) and perpendicular hereto (XZ plane). In both pericytes and astrocytes, ceruloplasmin and hephaestin are seen primarily at the cellular membrane. Both proteins are seen above and below the nuclei and exhibit both a luminal and abluminal distribution. Nuclei are stained with DAPI. *Scale bar* = 10 μm

endothelial cells in vivo. The cultured barrier-forming RBECs thus disclose important findings relevant for the understanding of iron transport of the BBB in vivo.

Distribution of Iron-Related Genes and Proteins in Brain Endothelial Cells

Iron binds to transferrin with high affinity in blood plasma [7], but transferrin is not able to enter the brain due to its hydrophilic nature. Therefore, the brain endothelial cells express receptors for transferrin on their luminal site [1]. This is a unique feature of the brain, since it is the only organ that expresses these receptors on its endothelial cells [52, 53]. The transferrin receptor of the brain endothelial cells has high affinity for holotransferrin [54]. In the present study, the expression of the transferrin receptor 1 was down-regulated once the cells were grown in polarized conditions. This observation is consistent with previous observations that the transferrin receptor is more expressed by proliferating cells compared to non-proliferating cells [54]. The transferrin receptor is regulated by iron supply [54], although this pattern is not seen in brain endothelial cells [55]. Increased expression of the transferrin receptor during iron deficiency was found in total brain, liver, and duodenal mucosa. However, no difference was found in the brain capillaries, suggesting that instead of increasing the transferrin receptor expression, brain endothelial cells compensate during iron deficiency by increasing the cycling rate of transferrin receptors within the endosomes [16, 55].

To enable DMT1-mediated pumping of ferrous iron out of the endosome, ferric iron must be reduced. Steap 2 and 3 were suggested as good candidates for ferric reductase activity within brain endothelial cells [22]. These Steap proteins have not been widely studied leaving references to other studies limited. Expression of both Steap 2 and 3 was confirmed in RBE4s, RBECs, and in isolated brain capillaries, but the expression of Steap 2 was low, especially in the primary cells.

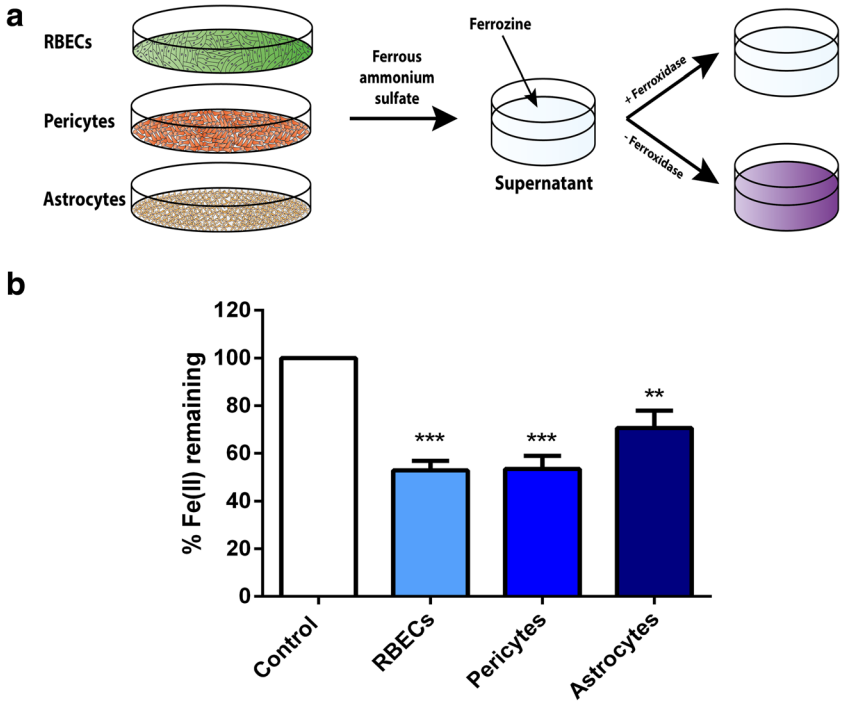

Fig. 6 Ferroxidase activity in cells of the neurovascular unit. **a** Schematic presentation of the ferroxidase assay. Confluent monolayers of RBECs, pericytes, and astrocytes were incubated with ferrous iron sulfate. The supernatants were analyzed for remaining ferrous iron sulfate using Ferrozine. When complexed with ferrous iron, Ferrozine develops into a purple-colored substance, but in the presence of oxidized iron, no color develops. **b** The ferrous activity in all cell types of the neurovascular unit is verified in this assay. The reduction of detectable ferrous ammonium sulfate indicates ferroxidase activity due to the presence of ceruloplasmin and hephaestin in the three cell types. Data are presented as means ± SEM ($n = 6$). $^{**}p < 0.01$,$^{***}p < 0.001$, and * indicate significant differences from control

In vivo studies were unable to detect the expression of DMT1 in the brain capillaries [15, 16, 56], while other studies detected DMT1 expression both in vivo [20, 37, 39] and in cultured immortalized RBECs [23]. DMT1 expression was observed in both RBE4s and RBECs, confirmed by both gene and protein expression analysis. DMT1 gene expression was, additionally, found in isolated brain capillaries. Immunocytochemical staining of DMT1 revealed distribution in a punctuated manner within the cell cytoplasm, which corresponds to the immunohistochemical staining previously found in neurons [16]. The in vitro experiments of the current study indicate that it is possible to detect DMT1 in primary RBECs in spite of the fact that prior studies failed to detect DMT1 in RBECs in vivo [16]. Hence, although substantial DMT1 immunoreactivity is present in neurons in sharp contrast to that of brain endothelial cells in vivo, it is likely that perturbed function of DMT1 in brain endothelial cells plays a role for the decreased iron transport into the brain occurring in the Belgrade rat suffering from a mutation in DMT1 [16].

Ferroportin was detected within isolated brain capillaries and RBECs, which correspond to previous observations [21, 22, 35, 36, 40]. Immunocytochemical staining of ferroportin would mainly be expected to occur near the abluminal cell membrane, since this protein is responsible for the transport of iron out of the cell cytoplasm. We observed immunocytochemical staining for ferroportin at the abluminal cell membrane and within the cytosol displaying a punctate immunoreactivity, which corresponds to the distribution observed in human brain microvascular cells [35].

Ferroportin has binding capacity for hepcidin, and a recent study determined the influence of hepcidin on efflux of iron from endothelial cells [22]. Supporting these observations, retention of radiolabeled iron occurred within the primary RBECs following hepcidin exposure [57]. Together these data indicate that hepcidin can access the endothelial ferroportin and negatively affect the efflux of iron. The evidence for hepcidin in brain endothelial cells is scarce [33, 49], which also is the clear impression derived from the data of the present study. It may thus be questioned whether hepcidin plays a role for ferroportin-mediated iron efflux from brain endothelial cells in physiological conditions. Conversely, in conditions with circulatory iron overloading where hepcidin is abundant in blood plasma and in conditions with cerebral pathology and a compromised BBB, hepcidin may indeed affect the iron efflux and prevent transport from brain endothelial cells further into the brain [33], hence protecting the neurons from the susceptibility of oxidative stress caused by iron excess.

Brain Endothelial Cells, Pericytes, and Astrocytes Express Both Forms of Ceruloplasmin and Hephaestin

Supporting that the detachment of iron from transferrin occurs within the brain endothelial cells, we identified that both pericytes and astrocytes express soluble and GPI-anchored forms of ceruloplasmin. The expression of ceruloplasmin in astrocytes is well-known [14]. Less characterized is the expression of ceruloplasmin and hephaestin in the NVU, but the proteins were recently detected in a brain endothelial cell line [35]. Notably, the expression of hephaestin was higher than ceruloplasmin in RBECs, whereas the opposite applied to these proteins concerning their expression in pericytes and astrocytes. In the context of release of ferrous iron from the abluminal side of brain endothelial cells, it is especially relevant that pericytes express the soluble form of ceruloplasmin, as the protein is capable of diffusing with limited distance to the brain endothelial cells to support the latter with ferroxidase activity. That brain endothelial cells, pericytes, and astrocytes all express GPI-anchored ceruloplasmin and hephaestin also supports the observation that these cells generate intracellular ferroxidase activity.

The subcellular distribution of hephaestin was localized to both the cellular membrane and cytoplasm, which is somewhat similar to that reported previously by McCarthy and colleagues [35], who mainly observed the protein near the cellular membrane. Yang and colleagues [36] detected a faint staining for hephaestin in pericytes, when using the same protocol for isolation of pericytes and the same anti-hephaestin antibody as used in the present study. They also detected expression of the hephaestin gene in pericytes, but their expression was lower than seen in brain endothelial cells, which is in good accordance with our observations.

A Model for Transport of Iron Through the Blood-Brain Barrier and Neurovascular Unit

Two different theories have evolved in order to explain the mechanism by which iron is transported into the brain. In this study, we report that RBECs express all the relevant proteins needed for iron uptake by the transferrin receptor, endocytosis, ferrireductase activity, and DMT1-mediated translocation of iron across the endosomal membrane and finally ferroportin mediated iron release from the cell cytoplasm to the brain parenchyma. The apo-transferrin receptor complex is then recycled to the luminal membrane at where apo-transferrin is released from the transferrin receptor. Although it should be noted that the data of the present study cannot discard the hypotheses on transcytosis of iron-transferrin through brain endothelial cells, the concerted expression of Steap, DMT1, and ferroportin suggests that iron is detached from transferrin within the brain endothelium. Moreover, the detection of mainly hephaestin in RBECs and ceruloplasmin in pericytes and astrocytes suggests that the NVU provides the necessary ferroxidase activity needed to convert ferrous iron to ferric iron. The resulting apo-transferrin within brain endothelial cells has higher affinity for its receptor at lower pH and would therefore be recycled to the plasma, while iron would enter the brain interstitium and undergo binding to transferrin or citrate present in the interstitial fluid [1]. We have summarized these

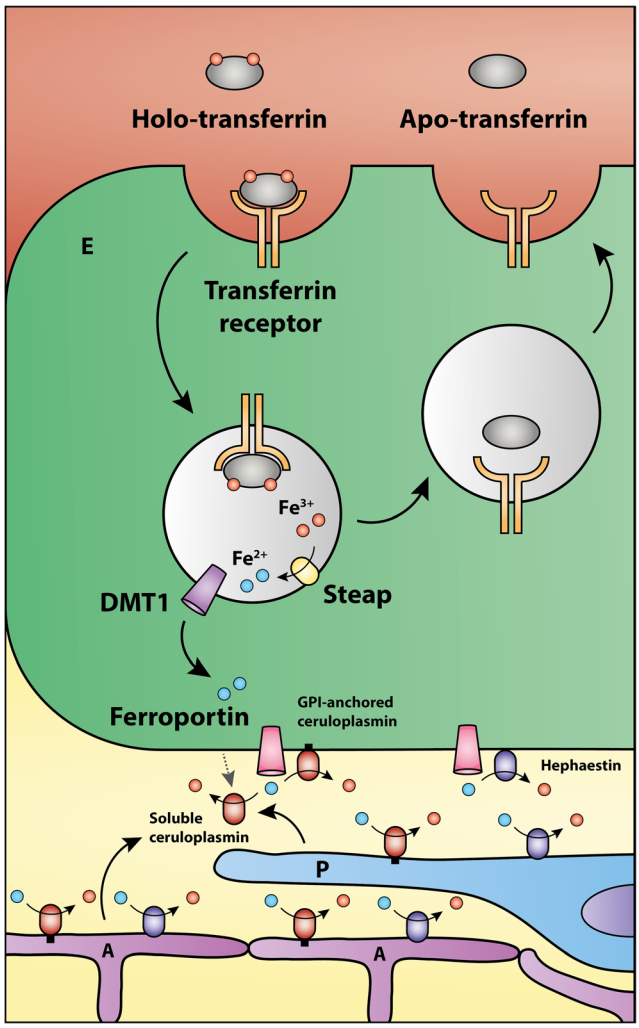

Fig. 7 A proposed model for iron transport across the blood-brain barrier. Holo-transferrin binds to transferrin receptors on the luminal side of the brain endothelial cell (*E*), and the complex becomes internalized in endosomes. The pH within the endosomes decreases, causing a dissociation of ferric iron (Fe^{3+}) from transferrin. Ferrireductases, like the six-transmembrane epithelial antigen of prostate (*Steap*) proteins, reduce ferric iron to ferrous iron (Fe^{2+}), which is translocated across the endosomal membrane to the cytosol by divalent metal transporter 1 (*DMT1*). The transferrin receptor and apo-transferrin are recycled to the luminal membrane. Ferrous iron is transported out of the cytosol by means of the transmembrane protein ferroportin. Ferroxidase activity is provided by the GPI-anchored forms of ceruloplasmin and by hephaestin that both are expressed by RBECs and by the soluble form of ceruloplasmin secreted from pericytes (*P*) and astrocytes (*A*). Pericytes and astrocytes also express GPI-anchored ceruloplasmin and hephaestin corresponding to their intracellular ferroxidase activity

observations and relevant conclusions in a separate figure (Fig. 7). A new study suggests that transferrin of the brain interstitium is capable of being internalized at the abluminal side of the brain endothelial cells [46]. This could imply that the saturation of the transferrin in the brain interstitium is of importance for the amount of iron being transported through brain endothelial cells.

In summary, we show that polarized primary brain endothelial cells express all the necessary proteins for ferric iron to be taken up by the transferrin receptor 1 by receptor-mediated endocytosis, reduced to ferrous iron by ferrireductases, translocated to the cytosol by DMT1, and pumped out of the cytosol by ferroportin. Pericytes, in addition to brain endothelial cells and astrocytes, expressed ceruloplasmin and hephaestin and thereby likely to provide the necessary ferroxidase activity needed for ferroportin-mediated iron release in the brain parenchyma.

Acknowledgments The Research Initiative on Blood-Brain Barrier and Drug Delivery founded by the Lundbeck foundation (Grant no. 2013-14113), The Danish Innovation Fund (Grant no. 014-2011-5), and Fonden til Lægevidenskabens Fremme are all thanked for generous support. We thank Merete Fredsgaard, Mathias Buhl Blæsild and Hanne Krone Nielsen, Aalborg University, Denmark for excellent technical assistance.

References

1. Moos T, Rosengren NT, Skjorringe T, Morgan EH (2007) Iron trafficking inside the brain. J Neurochem 103:1730–1740
2. Rouault TA (2013) Iron metabolism in the CNS: implications for neurodegenerative diseases. Nat Rev Neurosci 14:551–564
3. Ward RJ, Zucca FA, Duyn JH, Crichton RR, Zecca L (2014) The role of iron in brain ageing and neurodegenerative disorders. Lancet Neurol 13:1045–1060
4. Anderson GJ, Vulpe CD (2009) Mammalian iron transport. Cell Mol Life Sci 66:3241–3261
5. Abbott NJ, Patabendige AA, Dolman DE, Yusof SR, Begley DJ (2010) Structure and function of the blood-brain barrier. Neurobiol Dis 37:13–25
6. Dautry-Varsat A (1986) Receptor-mediated endocytosis: the intracellular journey of transferrin and its receptor. Biochimie 68:375–381
7. Morgan EH (1983) Effect of pH and iron content of transferrin on its binding to reticulocyte receptors. Biochim Biophys Acta 762: 498–502
8. Fleming MD, Romano MA, Su MA, Garrick LM, Garrick MD, Andrews NC (1998) Nramp2 is mutated in the anemic Belgrade (b) rat: evidence of a role for Nramp2 in endosomal iron transport. Proc Natl Acad Sci U S A 95:1148–1153
9. Ohgami RS, Campagna DR, Greer EL, Antiochos B, McDonald A, Chen J, Sharp JJ, Fujiwara Y et al (2005) Identification of a ferrireductase required for efficient transferrin-dependent iron uptake in erythroid cells. Nat Genet 37:1264–1269
10. Abboud S, Haile DJ (2000) A novel mammalian iron-regulated protein involved in intracellular iron metabolism. J Biol Chem 275:19906–19912
11. Anderson GJ, Frazer DM, McKie AT, Vulpe CD (2002) The ceruloplasmin homolog hephaestin and the control of intestinal iron absorption. Blood Cells Mol Dis 29:367–375
12. Patel BN, Dunn RJ, Jeong SY, Zhu Q, Julien JP, David S (2002) Ceruloplasmin regulates iron levels in the CNS and prevents free radical injury. J Neurosci 22:6578–6586
13. Petrak J, Vyoral D (2005) Hephaestin—a ferroxidase of cellular iron export. Int J Biochem Cell Biol 37:1173–1178
14. Patel BN, David S (1997) A novel glycosylphosphatidylinositol-anchored form of ceruloplasmin is expressed by mammalian astrocytes. J Biol Chem 272:20185–20190
15. Moos T, Morgan EH (2004) The significance of the mutated divalent metal transporter (DMT1) on iron transport into the Belgrade rat brain. J Neurochem 88:233–245
16. Moos T, Skjoerringe T, Gosk S, Morgan EH (2006) Brain capillary endothelial cells mediate iron transport into the brain by segregating iron from transferrin without the involvement of divalent metal transporter 1. J Neurochem 98:1946–1958
17. Boserup MW, Lichota J, Haile D, Moos T (2011) Heterogenous distribution of ferroportin-containing neurons in mouse brain. Biometals 24:357–375
18. Crowe A, Morgan EH (1992) Iron and transferrin uptake by brain and cerebrospinal fluid in the rat. Brain Res 592:8–16
19. Strahan ME, Crowe A, Morgan EH (1992) Iron uptake in relation to transferrin degradation in brain and other tissues of rats. Am J Physiol 263:R924–9
20. Burdo JR, Menzies SL, Simpson IA, Garrick LM, Garrick MD, Dolan KG, Haile DJ, Beard JL et al (2001) Distribution of divalent metal transporter 1 and metal transport protein 1 in the normal and Belgrade rat. J Neurosci Res 66:1198–1207
21. Wu LJ, Leenders AG, Cooperman S, Meyron-Holtz E, Smith S, Land W, Tsai RY, Berger UV et al (2004) Expression of the iron transporter ferroportin in synaptic vesicles and the blood-brain barrier. Brain Res 1001:108–117
22. McCarthy RC, Kosman DJ (2014) Glial cell ceruloplasmin and hepcidin differentially regulate iron efflux from brain microvascular endothelial cells. PLoS One 9:e89003
23. McCarthy RC, Kosman DJ (2012) Mechanistic analysis of iron accumulation by endothelial cells of the BBB. Biometals 25:665–675
24. Nakagawa S, Deli MA, Kawaguchi H, Shimizudani T, Shimono T, Kittel A, Tanaka K, Niwa M (2009) A new blood-brain barrier model using primary rat brain endothelial cells, pericytes and astrocytes. Neurochem Int 54:253–263
25. Burkhart A., Thomsen L. B., Thomsen M. S., Lichota J., Fazakas C., Krizbai I., Moos T. (2015) Transfection of brain capillary endothelial cells in primary culture with defined blood-brain barrier properties. Fluids Barriers CNS. 12, 19-015-0015-9
26. Laskey J, Webb I, Schulman HM, Ponka P (1988) Evidence that transferrin supports cell proliferation by supplying iron for DNA synthesis. Exp Cell Res 176:87–95
27. Thomsen M. S., Andersen M. V., Christoffersen P. R., Jensen M. D., Lichota J. and Moos T., (2015) Neurodegeneration with inflammation is accompanied by accumulation of iron and ferritin in microglia and neurons. Neurobiol Dis
28. Roux F, Durieu-Trautmann O, Chaverot N, Claire M, Mailly P, Bourre JM, Strosberg AD, Couraud PO (1994) Regulation of gamma-glutamyl transpeptidase and alkaline phosphatase activities in immortalized rat brain microvessel endothelial cells. J Cell Physiol 159:101–113
29. Rubin LL, Hall DE, Porter S, Barbu K, Cannon C, Horner HC, Janatpour M, Liaw CW et al (1991) A cell culture model of the blood-brain barrier. J Cell Biol 115:1725–1735
30. Wilhelm I, Fazakas C, Krizbai IA (2011) In vitro models of the blood-brain barrier. Acta Neurobiol Exp (Wars) 71:113–128

31. Pfaffl MW (2001) A new mathematical model for relative quantification in real-time RT-PCR. Nucleic Acids Res 29:e45
32. Gosk S, Vermehren C, Storm G, Moos T (2004) Targeting anti-transferrin receptor antibody (OX26) and OX26-conjugated liposomes to brain capillary endothelial cells using in situ perfusion. J Cereb Blood Flow Metab 24:1193–1204
33. Urrutia P, Aguirre P, Esparza A, Tapia V, Mena NP, Arredondo M, Gonzalez-Billault C, Nunez MT (2013) Inflammation alters the expression of DMT1, FPN1 and hepcidin, and it causes iron accumulation in central nervous system cells. J Neurochem 126:541–549
34. Wong BX, Tsatsanis A, Lim LQ, Adlard PA, Bush AI, Duce JA (2014) Beta-amyloid precursor protein does not possess ferroxidase activity but does stabilize the cell surface ferrous iron exporter ferroportin. PLoS One 9:e114174
35. McCarthy RC, Kosman DJ (2013) Ferroportin and exocytoplasmic ferroxidase activity are required for brain microvascular endothelial cell iron efflux. J Biol Chem 288:17932–17940
36. Yang WM, Jung KJ, Lee MO, Lee YS, Lee YH, Nakagawa S, Niwa M, Cho SS et al (2011) Transient expression of iron transport proteins in the capillary of the developing rat brain. Cell Mol Neurobiol 31:93–99
37. Burdo JR, Simpson IA, Menzies S, Beard J, Connor JR (2004) Regulation of the profile of iron-management proteins in brain microvasculature. J Cereb Blood Flow Metab 24:67–74
38. Moos T, Morgan EH (2001) Restricted transport of anti-transferrin receptor antibody (OX26) through the blood-brain barrier in the rat. J Neurochem 79:119–129
39. Siddappa AJ, Rao RB, Wobken JD, Leibold EA, Connor JR, Georgieff MK (2002) Developmental changes in the expression of iron regulatory proteins and iron transport proteins in the perinatal rat brain. J Neurosci Res 68:761–775
40. McCarthy RC, Park YH, Kosman DJ (2014) sAPP modulates iron efflux from brain microvascular endothelial cells by stabilizing the ferrous iron exporter ferroportin. EMBO Rep 15:809–815
41. Gaillard PJ, de Boer AG (2000) Relationship between permeability status of the blood-brain barrier and in vitro permeability coefficient of a drug. Eur J Pharm Sci 12:95–102
42. Skjorringe T, Burkhart A, Johnsen KB, Moos T (2015) Divalent metal transporter 1 (DMT1) in the brain: implications for a role in iron transport at the blood-brain barrier, and neuronal and glial pathology. Front Mol Neurosci 8:19
43. McKie AT, Barrow D, Latunde-Dada GO, Rolfs A, Sager G, Mudaly E, Mudaly M, Richardson C et al (2001) An iron-regulated ferric reductase associated with the absorption of dietary iron. Science 291:1755–1759
44. Stewart PA, Beliveau R, Rogers KA (1996) Cellular localization of P-glycoprotein in brain versus gonadal capillaries. J Histochem Cytochem 44:679–685
45. Roberts RL, Fine RE, Sandra A (1993) Receptor-mediated endocytosis of transferrin at the blood-brain barrier. J Cell Sci 104(Pt 2): 521–532
46. Simpson IA, Ponnuru P, Klinger ME, Myers RL, Devraj K, Coe CL, Lubach GR, Carruthers A et al (2015) A novel model for brain iron uptake: introducing the concept of regulation. J Cereb Blood Flow Metab 35:48–57
47. Zhang DL, Hughes RM, Ollivierre-Wilson H, Ghosh MC, Rouault TA (2009) A ferroportin transcript that lacks an iron-responsive element enables duodenal and erythroid precursor cells to evade translational repression. Cell Metab 9:461–473
48. Ward DM, Kaplan J (2012) Ferroportin-mediated iron transport: expression and regulation. Biochim Biophys Acta 1823:1426–1433
49. Wang SM, Fu LJ, Duan XL, Crooks DR, Yu P, Qian ZM, Di XJ, Li J et al (2010) Role of hepcidin in murine brain iron metabolism. Cell Mol Life Sci 67:123–133
50. Vulpe CD, Kuo YM, Murphy TL, Cowley L, Askwith C, Libina N, Gitschier J, Anderson GJ (1999) Hephaestin, a ceruloplasmin homologue implicated in intestinal iron transport, is defective in the sla mouse. Nat Genet 21:195–199
51. Patel BN, Dunn RJ, David S (2000) Alternative RNA splicing generates a glycosylphosphatidylinositol-anchored form of ceruloplasmin in mammalian brain. J Biol Chem 275:4305–4310
52. Jefferies WA, Brandon MR, Hunt SV, Williams AF, Gatter KC, Mason DY (1984) Transferrin receptor on endothelium of brain capillaries. Nature 312:162–163
53. Angelova-Gateva P (1980) Iron transferrin receptors in rat and human cerebrum. Agressologie 21:27–30
54. Moos T, Morgan EH (2000) Transferrin and transferrin receptor function in brain barrier systems. Cell Mol Neurobiol 20:77–95
55. Moos T, Oates PS, Morgan EH (1998) Expression of the neuronal transferrin receptor is age dependent and susceptible to iron deficiency. J Comp Neurol 398:420–430
56. Gunshin H, Mackenzie B, Berger UV, Gunshin Y, Romero MF, Boron WF, Nussberger S, Gollan JL et al (1997) Cloning and characterization of a mammalian proton-coupled metal-ion transporter. Nature 388:482–488
57. Burkhart A. (2014) The blood-brain barrier in vitro using primary culture: implications for studies of therapeutic gene expression and iron transport. PhD thesis, River Publishers, Aalborg, pp. 136